

Gd₂OsC₂, a soft ferromagnet with a surprisingly high Curie temperature and other rare-earth osmium and rhenium carbides with Pr₂ReC₂ type structure

Martin H. Gerdes, Wolfgang Jeitschko*, Klaus H. Wachtmann and Martin E. Danebrock

Anorganisch-Chemisches Institut, Universität Münster, Wilhelm-Klemm-Straße 8, D-48149 Münster, Germany

The six new carbides Ln₂OsC₂ (Ln = Y, Gd–Er) have been prepared by arc-melting cold-pressed pellets of the elemental components with subsequent annealing. They crystallize in the orthorhombic Pr₂ReC₂ structure (*Pnma*, *Z* = 4), which was refined from powder diffractometer data of Tb₂OsC₂. Chemical bonding in these carbides is discussed. The magnetic susceptibilities of the compounds Ln₂OsC₂ (Ln = Y, Gd and Tb) have been investigated with a SQUID magnetometer between 2 and 400 K with magnetic flux densities up to 5.5 T. The magnetic susceptibility of Y₂OsC₂ is low and almost temperature independent, suggesting Pauli paramagnetism. Gd₂OsC₂ and Tb₂OsC₂ are ferromagnetic with the relatively high Curie temperatures of 320 ± 5 and 210 ± 5 K, respectively. The gadolinium compound has the rather low coercivity of 23.8 ± 0.4 A cm⁻¹ at room temperature and 31.8 ± 0.8 A cm⁻¹ at 5 K. The magnetic properties of the corresponding rhenium carbides Ln₂ReC₂ (Ln = Ce, Pr, Nd, Gd, Tm) were also determined, thus completing the magnetic characterization of the rhenium series. The cerium atoms in Ce₂ReC₂ show mixed-valence behaviour. Antiferromagnetic order was observed for the moments of the rare-earth atoms in Pr₂ReC₂, *T_N* = 32 ± 2 K; Nd₂ReC₂, *T_N* = 42 ± 2 K; Gd₂ReC₂, *T_N* = 100 ± 5 K and Tm₂ReC₂, *T_N* = 5 ± 3 K.

The series of isotypic rare earth rhenium carbides with the compositions Ln₂ReC₂ (Ln = Y, Ce–Nd, Sm, Gd–Tm, Lu) was reported some time ago.¹ The crystal structure of these compounds was determined first from Guinier powder data of Pr₂ReC₂ and Y₂ReC₂, and confirmed by a single-crystal structure refinement from X-ray data of Er₂ReC₂.¹ The preparation of the ytterbium compound was communicated only recently.² The magnetic properties of these compounds were investigated by magnetic susceptibility measurements and by neutron diffraction. The rhenium atoms do not carry magnetic moments. The moments of the terbium, dysprosium, holmium and erbium atoms show antiferromagnetic order, all with Néel temperatures of < 100 K.^{3,4} Yb₂ReC₂ follows the Curie–Weiss law with no magnetic order above 2 K.²

In the present paper we report for the first time carbides of this structure type with osmium as the transition metal component. In contrast to the antiferromagnetism observed for the rhenium compounds, we found ferromagnetic order of the rare-earth moments in Gd₂OsC₂ and Tb₂OsC₂. We also report on the magnetic properties of those rhenium compounds which have not been investigated before.

Experimental

Starting materials for the preparation of the ternary carbides were ingots of the rare-earth metals and powders of rhenium (H. C. Starck) and osmium (Degussa), all with nominal purities > 99.9%. Graphite was purchased in the form of flakes (Alpha, > 99.5%, 20 mesh). Filings of the rare-earth metals were prepared under dried (Na) paraffin oil, which was washed away by dry hexane prior to the sample preparation. Adhering iron particles were removed with a magnet. The filings were stored under argon and were only briefly exposed to air prior to the reactions. The more reactive rare-earth elements, including gadolinium, were used in the form of small pieces.

The samples were prepared by arc-melting of small (300–400 mg), cold-pressed pellets of the elemental components with the ideal composition in an argon (> 99.996%) atmosphere. A titanium button was repeatedly melted prior to the reactions to further purify the argon. The samples were melted from both sides to enhance their homogeneity. They were then wrapped in tantalum foil and annealed in evacuated silica tubes for 30 days at 900 °C. Energy dispersive X-ray

fluorescence analyses of the samples did not show any impurity elements heavier than sodium (detectability limit approximately 1 atom%).

Guinier powder diagrams of the samples were recorded with Cu-Kα₁ radiation and α-quartz (*a* = 491.30, *c* = 540.46 pm) as an internal standard. The crystal structure of Tb₂OsC₂ was refined by the Rietveld method from powder diffractometer data (STOE, Stadi P), recorded with Ge(111)-monochromated Cu-Kα₁ radiation, a flat, rotating sample in the transmission mode and a linear position-sensitive detector. The refinement was carried out with the program FULLPROF.⁵ As starting positional parameters those obtained for Pr₂ReC₂ were used.¹ A total of 22 variable parameters was refined: the scale factor, ten atomic position parameters, three isotropic displacement parameters, the three cell parameters, the zero-point and four profile fitting parameters. Because of the low scattering power of the carbon atoms their displacement parameters oscillated with large standard deviations and we assumed they should be similar to those found for the other atoms of Tb₂OsC₂ and also similar to those of Er₂ReC₂.¹ Hence, they were not allowed to vary during the last least-squares refinement cycles.

The magnetic susceptibilities of polycrystalline samples were measured in the temperature range between 2 and 400 K with magnetic flux densities up to 5.5 T using a SQUID magnetometer (Quantum Design, MPMS). The samples were cooled in zero field and the susceptibilities were recorded continuously on heating.

Results and Discussion

The osmium containing compounds are reported here for the first time. They were already observed in the arc-melted, quenched samples. Nevertheless, the ingots were annealed to enhance their homogeneity.

Compact samples are stable in air for long periods of time. They have a light grey colour with metallic lustre; the powders are dark grey. The lattice constants of the carbides (Table 1) were obtained by least-squares fits of the Guinier powder data. The plot of the cell volumes of the carbides Ln₂ReC₂ and Ln₂OsC₂ (Fig. 1) shows the expected lanthanoid contraction.

Crystal structure of Tb₂OsC₂

The structure refinement of Tb₂OsC₂ from the diffractometer powder data resulted in a conventional residual of *R_F* = 0.081

Table 1 Lattice constants of carbides with the orthorhombic Pr_2ReC_2 structure^a

compound	<i>a</i> /pm	<i>b</i> /pm	<i>c</i> /pm	<i>V</i> /nm ³
Y_2OsC_2	645.0(1)	508.96(8)	978.0(1)	0.3211
Gd_2OsC_2	646.34(8)	517.82(5)	988.6(1)	0.3309
Tb_2OsC_2	643.82(8)	512.62(7)	981.0(1)	0.3238
Dy_2OsC_2	642.4(2)	509.7(1)	975.3(2)	0.3193
Ho_2OsC_2	641.28(5)	506.88(5)	971.37(8)	0.3157
Er_2OsC_2	640.45(4)	503.41(5)	966.68(8)	0.3117

^aStandard deviations in the values of the last listed digits are given in parentheses throughout the paper.

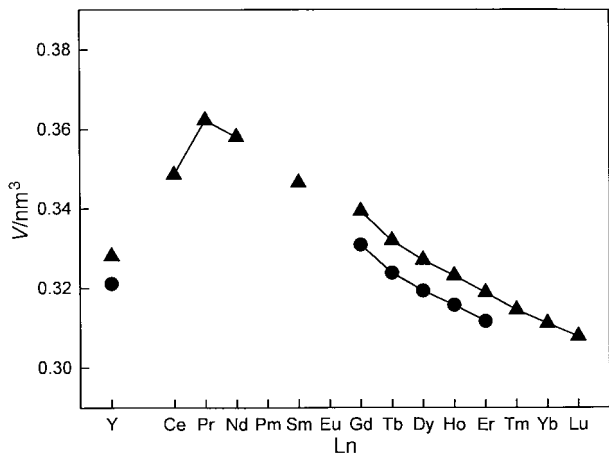


Fig. 1 Cell volumes of Pr_2ReC_2 type carbides (\blacktriangle , Ln_2ReC_2 ; \bullet , Ln_2OsC_2)

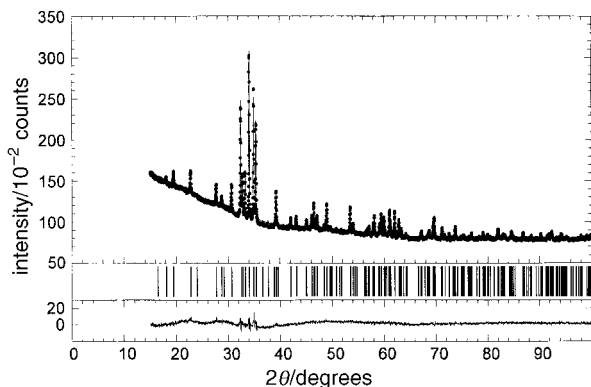


Fig. 2 Rietveld refinement plots for Tb_2OsC_2 . The data were recorded with $\text{Cu-K}\alpha_1$ radiation. The top profile shows the observed counts (dots) superimposed with the trace of the calculated pattern. The calculated positions of the Bragg reflections and the difference profile are also shown.

for the 190 independent structure factors with 22 variable parameters. The quality of the refinement may be judged by comparing the profile with the difference profile (Fig. 2). The resulting atomic parameters and the interatomic distances are listed in Tables 2 and 3. A projection of the structure is shown in Fig. 3.

The structure refinement of Tb_2OsC_2 confirms that this compound is isotypic with Pr_2ReC_2 and Er_2ReC_2 , although the positional parameters of Tb_2OsC_2 resulting from the powder refinement are not as accurate as the parameters obtained from the earlier structure determination of Er_2ReC_2 from single-crystal data.¹

The crystal structure of Er_2ReC_2 has already been discussed.¹ The terbium atoms are slightly larger than the erbium atoms, and osmium is slightly smaller than rhenium. The interatomic distances of Tb_2OsC_2 and Er_2ReC_2 reflect these differences,

Table 2 Atomic parameters of Tb_2OsC_2

atom	<i>Pnma</i>	<i>x</i>	<i>y</i>	<i>z</i>	<i>B</i> ^a
Tb(1)	4c	0.8129(4)	1/4	0.0512(2)	0.66(7)
Tb(2)	4c	0.4744(4)	1/4	0.7823(3)	0.48(7)
Os	4c	0.2745(3)	1/4	0.1363(2)	0.22(5)
C(1)	4c	0.029(7)	1/4	0.255(4)	0.5 ^a
C(2)	4c	0.689(6)	1/4	0.546(4)	0.5 ^a

^aThe isotropic displacement parameters *B* ($\times 10^4$ pm²) of the C(1) and C(2) positions were not refined.

Table 3 Interatomic distances in the structure of Tb_2OsC_2 ^a

Tb(1):	1C(1)	243.6	Os:	1C(2)	187.1
	2C(2)	256.4		1C(1)	195.5
	1C(2)	260.2		1C(1)	196.3
	1C(1)	263.7		1Tb(1)	307.6
	1Os	307.6		1Tb(1)	308.7
	1Os	308.7		2Tb(2)	313.4
	2Os	320.5		2Tb(1)	320.5
	1Tb(2)	342.2		2Tb(2)	334.5
	1Tb(2)	343.3		1Tb(1)	356.5
	2Tb(2)	355.8		1Tb(2)	370.4
	1Os	356.5		2Os	391.6
	2Tb(1)	365.8	C(1):	1Os	195.5
	2Tb(2)	368.6		1Os	196.3
Tb(2):	1C(2)	249.3		1Tb(1)	243.6
	2C(1)	257.7		2Tb(2)	257.7
	1C(2)	269.9		1Tb(1)	263.7
	2Os	313.4	C(2):	1Os	187.1
	2Tb(2)	328.1		1Tb(2)	249.3
	2Os	334.5		2Tb(1)	256.4
	1Tb(1)	342.2		1Tb(1)	260.2
	1Tb(1)	343.3		1Tb(2)	269.9
	2Tb(1)	355.8			
	2Tb(1)	368.6			
	1Os	370.4			

^aAll distances < 400 pm (Tb–Tb, Tb–Os, Tb–C, Os–Os, Os–C) and 300 pm (C–C) are listed. Standard deviations are all ≤ 0.4 pm for the metal–metal and ≤ 4 pm for the metal–carbon distances.

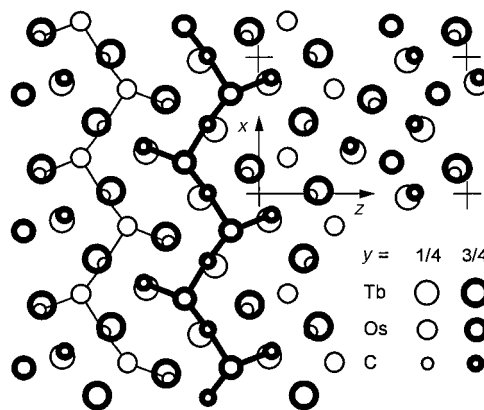


Fig. 3 The crystal structure of Tb_2OsC_2 . In the left-hand part of the drawing the one-dimensionally infinite, branched osmium–carbon polyanion is emphasized.

in spite of the relatively large standard deviations in the positional parameters of the carbon atoms. Thus, the average Tb(1)–C and Tb(2)–C distances of 256.1 and 258.7 pm are larger than the corresponding Er–C distances of 251.4 and 253.6 pm, and the average Os–C distance of 193.0 pm is smaller than the average Re–C distance of 197.6 pm.

Chemical bonding

It has been argued before, that the electron count for the rhenium atoms in Er_2ReC_2 is compatible with the 18-electron rule¹ and the same can be assumed for the osmium atoms in

Tb₂OsC₂. As is discussed below, and in agreement with this assumption, in both compounds the transition metal atoms do not carry magnetic moments.

An earlier extended Hückel calculation for the rhenium-carbon polyanion of Er₂ReC₂ had indicated that the highest occupied electronic states of the polyanion are antibonding.⁶ Since the occupation of antibonding states tends to destabilize a compound, it had been suggested that the Pr₂ReC₂ type carbides are stabilized by electron acceptors like hydrogen or small amounts of impurities on interstitial sites.⁶ The hydrogen content, however, can be ruled out, since the compounds, including the presently reported ternary osmium carbides, were prepared by arc-melting, and hydrides decompose at high temperatures. Also the structure refinements of the isotopic compounds Tb₂ReC₂ and Er₂ReC₂ from neutron diffraction data had shown that no significant amounts of impurity atoms could be present on interstitial sites.³ Furthermore, when a compound is stabilized by impurities one usually does not obtain single-phase products unless enough of the 'impurity' is added intentionally. Actually, the cell volume of Ce₂ReC₂ (Fig. 1) indicates that the rhenium-carbon polyanion in the Pr₂ReC₂ type carbides of the trivalent lanthanoids is electronically unsaturated, since the cell volume of the cerium compound deviates from the smooth function of the other Ln₂ReC₂ carbides, thus indicating that the cerium atoms are at least partially tetravalent in this compound. The electron count of the presently reported isotopic osmium compounds is also higher than that of the ternary rhenium carbides. All this indicates that the electrons at the Fermi level of Er₂ReC₂ do not occupy antibonding states.

For the extended Hückel calculation it had been assumed that the valence electrons of the lanthanoid atoms are completely transferred to the transition-metal-carbon polyanion. This assumption would exclude any bonding lanthanoid-lanthanoid interactions. We have argued earlier that these interactions should not be neglected.³ This is now further supported by the relatively short Tb-Tb distances of 328.1, 342.2, 343.3 and 355.8 pm in Tb₂OsC₂, which are all shorter than the average Tb-Tb distance of 356.6 pm calculated from the lattice constants of the hexagonal close-packed modification of elemental terbium.⁷ In this context it is of interest that the two shortest Tb-Tb distances of 328.1 and 342.2 pm in Tb₂OsC₂ are shorter than the two shortest Er-Er distances of 331.4 and 344.5 pm in Er₂ReC₂, even though the cell volume of Tb₂OsC₂ (0.3238 nm³) is larger than the cell volume of Er₂ReC₂ (0.3188 nm³). Thus, the higher electron count of the osmium compound enhances the bonding character of the Ln-Ln interactions. We have not been successful in preparing the osmium containing carbides with the early electropositive rare-earth elements (Ce, Pr, Nd), which could be obtained with rhenium as the transition-metal component (Fig. 1). This may be rationalized similarly: the large, electropositive lanthanoids would transfer a larger proportion of their valence electrons to the transition-metal-carbon polyanion, and these can be better accommodated in the rhenium compounds with the lower overall electron count.

Magnetic properties

Some magnetic properties of the Pr₂ReC₂ type carbides have already been reported.^{3,4} These investigations have shown that the rhenium atoms do not carry magnetic moments. This is also the case for the osmium atoms, as is demonstrated by Y₂OsC₂, where the yttrium atoms are not expected to carry magnetic moments. The magnetic susceptibility of this compound (Fig. 4) is essentially constant between 100 and 300 K, suggesting Pauli paramagnetism. The upturn of the magnetic susceptibility at lower temperature can be ascribed to paramagnetic impurities or to paramagnetic surface states. Nevertheless, we have also fitted these data to the modified Curie-Weiss law

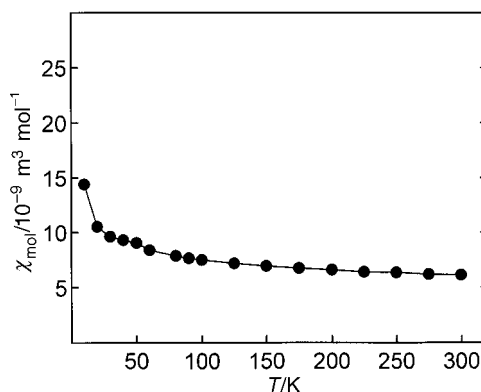


Fig. 4 The magnetic susceptibility of Y₂OsC₂ as a function of temperature, measured at a magnetic field strength of 1 T

$\chi = \chi_0 + C/(T - \Theta)$. The magnetic moment calculated from the resulting Curie constant according to $\mu_{\text{exp}} = 2.83 \sqrt{C} \mu_B = 0.18(4) \mu_B$ is very low, much smaller than the value of $1.73 \mu_B$ expected for one unpaired spin per formula unit. Hence, Pauli paramagnetism seems to be the correct assignment for this compound. The temperature independent value of the susceptibility obtained from the fit $\chi_0 = 5.2(1) \times 10^{-9} \text{ m}^3 \text{ mol}^{-1}$ is comparable to the Pauli paramagnetism of metals, e.g. for elemental palladium a susceptibility of $\chi = 6.9 \times 10^{-9} \text{ m}^3 \text{ mol}^{-1}$ has been reported.⁸

The temperature dependences of the reciprocal susceptibilities of Gd₂OsC₂ and Tb₂OsC₂ (Fig. 5) follow the Curie-Weiss law above 350 and 250 K, respectively. The positive Weiss constants of $\Theta = 316 \pm 5 \text{ K}$ for Gd₂OsC₂ and $\Theta = 169 \pm 5 \text{ K}$ for Tb₂OsC₂ indicate ferromagnetism. This was confirmed by the magnetization isotherms recorded at 5 K (Fig. 5). It can be seen that the hysteresis of the gadolinium compound is rather low with a coercivity of $H_c = 31.8 \pm 0.8 \text{ A cm}^{-1}$ and a remanence of $\mu_R = 0.078 \pm 0.002 \mu_B$ at 5 K. At 300 K the corresponding values are $H_c = 23.8 \pm 0.4 \text{ A cm}^{-1}$ and $\mu_R = 0.056 \pm 0.002 \mu_B$. Thus, this compound is a rather soft ferromagnet, however, not quite as soft as technically used soft magnets, e.g. electrical steel or amorphous iron alloys with coercivities⁹ varying between 10 and 0.01 A cm⁻¹. The Curie temperatures of Gd₂OsC₂ and Tb₂OsC₂ were determined as the turning points of the magnetization vs. temperature curves (not shown): $T_C = 320 \pm 5$ and $210 \pm 5 \text{ K}$, respectively. These values are rather high, considering that elemental gadolinium has a Curie temperature of $T_C = 292.7 \text{ K}$ and elemental terbium orders antiferromagnetically at a Néel temperature of $T_N = 230.2 \text{ K}$.¹⁰ At the highest magnetic flux densities accessible with our SQUID magnetometer the 'saturation' magnetizations of both compounds attain a value of $\mu_{\text{exp(sm)}} = 12.2 \pm 0.2 \mu_B$ per formula unit, i.e. $\mu_{\text{exp(sm)}} = 6.1 \pm 0.1 \mu_B/\text{Ln}^{3+}$. This value compares rather well with the theoretical values calculated from the relation $\mu_{\text{calc(sm)}} = gJ \mu_B$ (Table 4), considering that it was obtained from powder samples with random orientation of the easy axes of magnetization. The paramagnetic moments calculated from the slope of the $1/\chi$ vs. T plots at high temperatures are $\mu_{\text{exp}} = 6.3 \pm 0.3 \mu_B/\text{Gd}^{3+}$ and $\mu_{\text{exp}} = 9.4 \pm 0.1 \mu_B/\text{Tb}^{3+}$, respectively. These values are somewhat lower than the theoretical ones of $\mu_{\text{eff}} = 7.94 \mu_B/\text{Gd}^{3+}$ and $\mu_{\text{eff}} = 9.72 \mu_B/\text{Tb}^{3+}$ because the reciprocal susceptibilities of these compounds could not be measured at temperatures high enough to attain perfect linearity of the $1/\chi$ vs. T plots; this is especially true for the gadolinium compound with the relatively high Curie temperature.

The magnetic properties of the corresponding rhenium compounds Ln₂ReC₂ (Ln = Y, Tb, Dy, Ho, Er, Yb and Lu) have already been reported.²⁻⁴ Here we communicate the results for the remaining compounds with Ln = Ce, Pr, Nd, Gd and Tm. Table 5 gives a summary for all rhenium compounds.

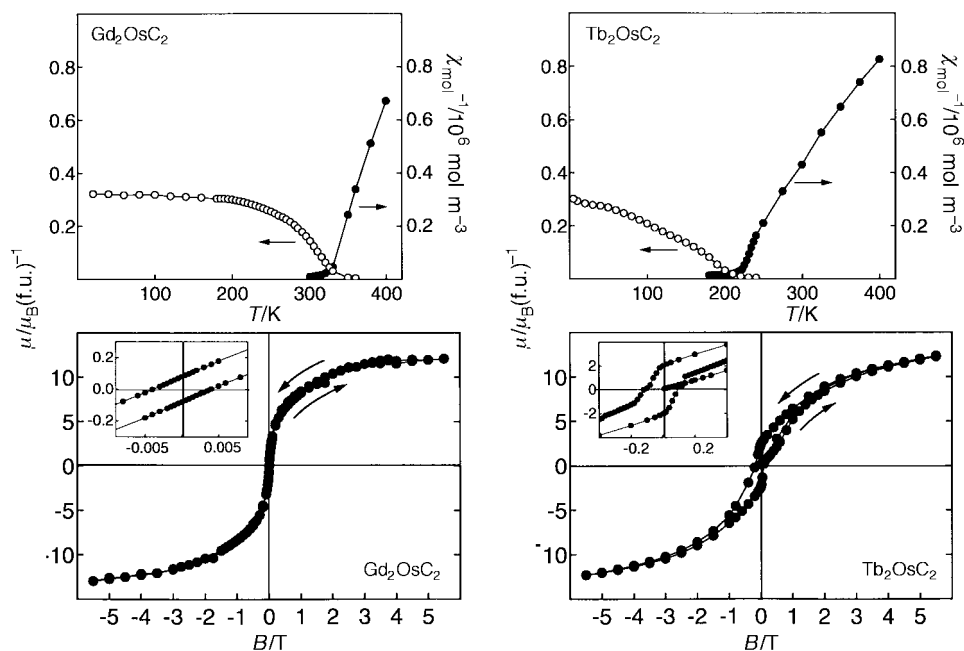


Fig. 5 Temperature dependence of the reciprocal susceptibilities and magnetization values of the ferromagnetic compounds Gd_2OsC_2 (left) and Tb_2OsC_2 (right) measured at a magnetic field strength of 0.01 T. The hysteresis loops of both compounds recorded at a temperature of 5 K are also shown.

Table 4 Magnetic properties of the carbides Ln_2OsC_2 ($\text{Ln}=\text{Y}, \text{Gd}, \text{Tb}$)^a

compound	magnetic property	$\mu_{\text{exp}}/\text{Ln}^{3+}$ (μ_{B})	$\mu_{\text{eff}}/\text{Ln}^{3+}$ (μ_{B})	Θ/K	T_{C}/K	$\mu_{\text{exp(sm)}}/\text{Ln}^{3+}$ (μ_{B})	$\mu_{\text{calc(sm)}}/\text{Ln}^{3+}$ (μ_{B})
Y_2OsC_2	Pauli paramagnetic	0	0	—	—	—	—
Gd_2OsC_2	ferromagnetic	6.3 ± 0.3	7.94	316 ± 5	320 ± 5	6.1 ± 0.1	7.0
Tb_2OsC_2	ferromagnetic	9.4 ± 0.1	9.72	169 ± 5	210 ± 5	6.1 ± 0.1	9.0

^aThe experimentally determined effective paramagnetic moments μ_{exp} obtained from $\mu_{\text{exp}}=2.83 [(\chi_{\text{cgs}}/2)(T-\Theta)]^{1/2} \mu_{\text{B}}$ are compared with the theoretical values $\mu_{\text{eff}}=g[J(J+1)]^{1/2} \mu_{\text{B}}$. The highest magnetic moments $\mu_{\text{exp(sm)}}$ reached in the magnetically ordered range (at 5 K) of the powder samples are given together with the theoretical values $\mu_{\text{calc(sm)}}$ for the Ln^{3+} ions, where $\mu_{\text{calc(sm)}}=gJ \mu_{\text{B}}$. The Weiss constants Θ and the Curie temperatures T_{C} are also listed.

Table 5 Magnetic properties of the carbides Ln_2ReC_2 ^a

compound	magnetic property	$\mu_{\text{exp}}/\text{Ln}^{3+}$ (μ_{B})	$\mu_{\text{eff}}/\text{Ln}^{3+}$ (μ_{B})	Θ/K	T_{N}/K	$\mu_{\text{exp(sm)}}/\text{Ln}^{3+}$ (μ_{B})	(T/K)	$\mu_{\text{calc(sm)}}/\text{Ln}^{3+}$ (μ_{B})	ref.
Y_2ReC_2	Pauli paramagnetic	—	0	—	—	—	—	0	3
Ce_2ReC_2	mixed valent	$(1.2 \pm 0.1)^b$	2.54	$(-8 \pm 1)^b$	—	—	—	2.14	this work
Pr_2ReC_2	metamagnetic	3.3 ± 0.2	3.58	4 ± 2	32 ± 2	0.33	30	3.2	this work
Nd_2ReC_2	metamagnetic	3.4 ± 0.2	3.62	13 ± 2	42 ± 2	0.33	37	3.27	this work
Gd_2ReC_2	antiferromagnetic	7.4 ± 0.2	7.94	60 ± 5	100 ± 5	—	—	7.0	this work
Tb_2ReC_2	metamagnetic	9.7 ± 0.2	9.72	67 ± 3	96 ± 2	4.4	70	9.0	3
Dy_2ReC_2	metamagnetic	10.3 ± 0.2	10.63	43 ± 3	58 ± 1	5.1	5	10.0	4
Ho_2ReC_2	metamagnetic	10.4 ± 0.2	10.60	21 ± 3	30 ± 1	6.1	5	10.0	4
Er_2ReC_2	metamagnetic	9.6 ± 0.2	9.58	22 ± 3	18 ± 1	5.4	5	9.0	3
Tm_2ReC_2	metamagnetic	7.2 ± 0.2	7.57	-5 ± 2	5 ± 3	2.3	2	7.0	this work
Yb_2ReC_2	paramagnetic	4.5 ± 0.1	4.54	-22 ± 1	< 2	—	—	4.0	2
Lu_2ReC_2	Pauli paramagnetic	—	0	—	—	—	—	0	3

^aListed are the Néel temperatures T_{N} and the highest magnetic moments $\mu_{\text{exp(sm)}}$ per Ln^{3+} ion reached for the metamagnetic compounds at the indicated temperatures with a magnetic flux density of 5.5 T. For comments concerning the headings of the other columns see Table 4. ^b See text.

The temperature dependences of the reciprocal susceptibilities of these latter carbides are plotted in Fig. 6. All compounds contained at least minor amounts of ferromagnetic impurities, as revealed by the field dependence of the susceptibility values. However, for the compounds with $\text{Ln}=\text{Pr}-\text{Tm}$ the impurity content was so low that the susceptibility values obtained at 3 and 5 T were practically the same, and therefore the values recorded at 5 T were used for the evaluations. Only in the case of Ce_2ReC_2 did we extrapolate to infinite magnetic field strengths. It can be seen that the temperature dependence of the reciprocal susceptibilities is linear above 150 K for all

compounds suggesting Curie–Weiss behaviour. The magnetic moments $\mu_{\text{exp}}/\text{Ln}^{3+}$ calculated from the slopes of these plots are in good agreement with the theoretically expected effective moments $\mu_{\text{eff}}/\text{Ln}^{3+}$ calculated from the relation $\mu_{\text{eff}}=g[J(J+1)]^{1/2} \mu_{\text{B}}$ (Table 5).

The only exception is the cerium compound. The calculation of the reciprocal susceptibility data of this compound according to the Curie–Weiss law resulted in a moment of $\mu_{\text{eff}}=1.2 \pm 0.1 \mu_{\text{B}}$ per cerium atom. This value is much lower than the theoretical value $\mu_{\text{eff}}=2.54 \mu_{\text{B}}$ for a Ce^{3+} atom, thus indicating a mixed or intermediate valence $\text{Ce}^{3+/4+}$ for the

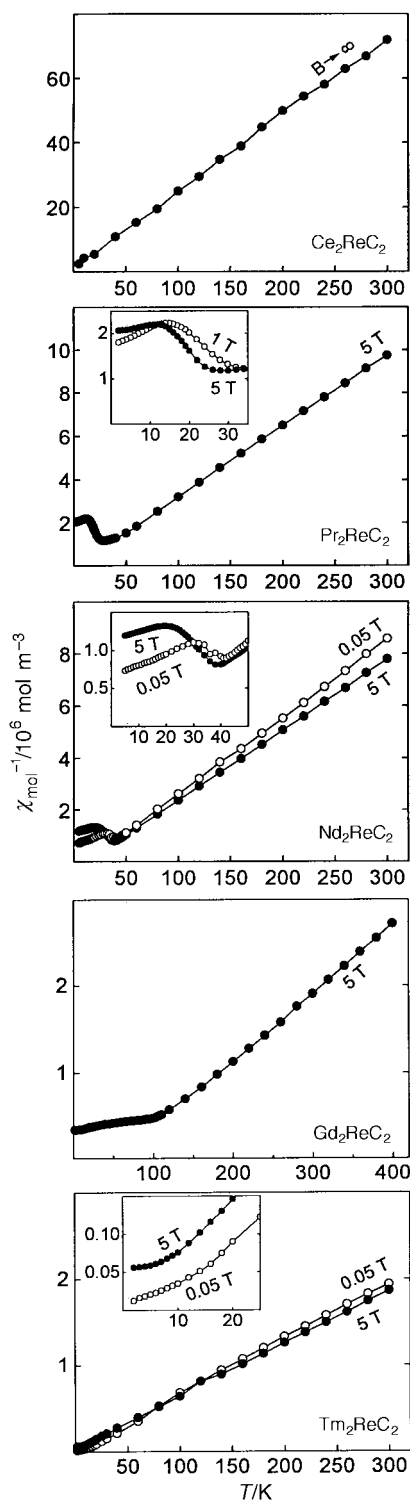


Fig. 6 Temperature dependence of the reciprocal susceptibilities of the carbides Ln_2ReC_2 ($\text{Ln}=\text{Ce}, \text{Pr}, \text{Nd}, \text{Gd}, \text{Tm}$ from top to bottom) measured at different magnetic field strengths. For the cerium compound the reciprocal susceptibility values shown were obtained by extrapolation to infinite external magnetic flux densities.

cerium atoms in Ce_2ReC_2 , since a Ce^{4+} ion should not carry a magnetic moment. At least partial tetravalent character can also be expected for the cerium atoms in Ce_2ReC_2 from the cell volume plot of the rhenium compounds (Fig. 1), as already discussed above. Since Ce_2ReC_2 is a mixed- or intermediate-valence compound the evaluation of the magnetic susceptibility data according to the Curie–Weiss law is not entirely correct,¹¹ however, since our sample of Ce_2ReC_2 contained a relatively large amount of a ferromagnetic impurity, we did not evaluate these data further.

At lower temperatures the $1/\chi$ vs. T plots of the compounds Ln_2ReC_2 ($\text{Ln}=\text{Pr}, \text{Nd}, \text{Gd}$ and Tm) indicate antiferromagnetic order. The Néel temperatures of these compounds vary between $T_N = 5 \pm 3$ K for the thulium compound and $T_N = 100 \pm 5$ K for the gadolinium compound (Table 5). Magnetization measurements for Gd_2ReC_2 below the Néel temperature showed a linear dependence of the magnetic moment with the external applied magnetic field, as is typical for a regular antiferromagnet. The magnetization isotherms of the other three compounds showed field dependences with weak transitions from the antiferromagnetic to the ferromagnetic states with increasing field strengths, as is typical for metamagnets.

We thank Dr. R.-D. Hoffmann for the collection of the powder diffractometer data, Dipl.-Chem. Th. Hüfken for the preparation and characterization of Dy_2OsC_2 and Mr. K. Wagner for investigating our samples in the scanning electron microscope. We are also grateful to Dr. G. Höfer (Heraeus Quarzschmelze), Dr. H. G. Nadler (H. C. Starck Co.) and Dr. W. Gerhartz (Degussa AG) for generous gifts of silica tubes and powders of rhenium and osmium, respectively. This work was also supported by the Deutsche Forschungsgemeinschaft and the Fonds der Chemischen Industrie.

References

- 1 W. Jeitschko, G. Block, G. E. Kahnert and R. K. Behrens, *J. Solid State Chem.*, 1990, **89**, 191.
- 2 R. Pöttgen, K. H. Wachtmann, W. Jeitschko, A. Lang and T. Ebel, *Z. Naturforsch., Teil B*, 1997, **52**, 231.
- 3 M. Reehuis, J. Rodriguez-Carvajal, M. E. Danebrock and W. Jeitschko, *J. Magn. Magn. Mater.*, 1995, **151**, 273.
- 4 M. Reehuis, M. E. Danebrock, J. Rodriguez-Carvajal, W. Jeitschko, N. Stüsser and R.-D. Hoffmann, *J. Magn. Magn. Mater.*, 1996, **154**, 355.
- 5 J. Rodriguez-Carvajal, FULLPROF: A Program for Rietveld Refinement and Profile Matching Analysis of Complex Powder Diffraction Patterns; Institut Laue-Langevin, 1991, unpublished work.
- 6 H. Deng and R. Hoffmann, *Inorg. Chem.*, 1993, **32**, 1991.
- 7 J. Donohue, *The Structures of the Elements*, Wiley, New York, 1974.
- 8 E. Vogt and M. Höhl, in *Landolt-Börnstein*, Springer, Berlin, 1962, 6th edn., vol. II/9, ch. 29, p. 5.
- 9 G. Herzer, in *Magnetwerkstoffe und Magnetsysteme*, ed. H. Warlimont, DGM Informationsgesellschaft, Oberursel, Germany, 1991, p. 143.
- 10 Gmelin, *Handbuch der anorganischen Chemie*, 8. Auflage, Seltenerdelemente, Teil B.3, Springer, Berlin, 1974, p. 306.
- 11 J. M. Lawrence, P. S. Riseborough and R. D. Parks, *Rep. Progr. Phys.*, 1981, **44**, 1.

Paper 7/03759G; Received 30th May, 1997